Cellular polarization: Interaction between extrinsic bounded noises and the wave-pinning mechanism

Sebastiano de Franciscis and Alberto d'Onofrio*

European Institute of Oncology, Department of Experimental Oncology, Via Ripamonti 435, I20141 Milano, Italy

(Received 19 December 2012; revised manuscript received 8 July 2013; published 11 September 2013)

Cell polarization (cued or uncued) is a fundamental mechanism in cell biology. As an alternative to the classical Turing bifurcation, it has been proposed that the onset of cell polarity might arise by means of the well-known phenomenon of wave-pinning [Gamba *et al.*, Proc. Natl. Acad. Sci. USA **102**, 16927 (2005)]. A particularly simple and elegant deterministic model of cell polarization based on the wave-pinning mechanism has been proposed by Edelstein-Keshet and coworkers [Biophys. J. **94**, 3684 (2008)]. This model consists of a small biomolecular network where an active membrane-bound factor interconverts into its inactive form that freely diffuses in the cell cytosol. However, biomolecular networks do communicate with other networks as well as with the external world. Thus, their dynamics must be considered as perturbed by extrinsic noises. These noises may have both a spatial and a temporal correlation, and in any case they must be bounded to preserve the biological meaningfulness of the perturbed parameters. Here we numerically show that the inclusion of external spatiotemporal bounded parametric perturbations in the above wave-pinning-based model of cellular polarization may sometimes destroy the polarized state. The polarization loss depends on both the extent of temporal and spatial correlations and on the kind of noise employed. For example, an increase of the spatial correlation of the noise induces an increase of the probability of cell polarization. However, if the noise is spatially homogeneous then the polarization is lost in the majority of cases. These phenomena are independent of the type of noise. Conversely, an increase of the temporal autocorrelation of the noise induces an effect that depends on the model of noise.

DOI: 10.1103/PhysRevE.88.032709 PACS number(s): 87.18.Tt

I. INTRODUCTION

The formation of two distinct spatial domains enabling two separate and distinct parts, let us say a "tail" and a "head," to be established in a single cell, is called cellular polarization [1]. This phenomenon lies at the basis of two fundamental bioprocesses: the asymmetric division of differentiating cells [2] and the chemotactic motion of certain kinds of cells (for example, neutrophils) [1].

As far as cell division is concerned, when a stem cell has divided, in the vast majority of cases the two daughter cells must be of two different types: one has to be a stem cell, and the other has to be a more differentiated cell. This kind of outcome of cell division is termed asymmetric division, by contrast with the case of symmetric division, where both the daughter cells belong to the same cellular type (e.g., both stem cells or both semidifferentiated cells). This implies that the proteins determining the cellular type must exhibit a spatial pattern of markedly different concentrations. The cell spatial pattern associated with asymmetric division has to regularly repeat until the replicating potential of the proliferating cell is exhausted (theoretically never for stem cells); thus, it is thought to be essentially *uncued* [3]. However, there are models, such as that by Ortoleva and Ross [4], that postulate a role of random cues for the onset of asymmetric cellular division.

Chemotaxis is the process by which some cells "sense" the gradient of a chemical—termed chemoattractant—and start moving along the direction of increasing concentration of the attractant. Chemorepulsion is instead the opposite process by which some cells move away from chemicals, i.e., the chemorepellors. As a consequence, unlike in the uncued phenomenon of asymmetric cell division, the spatial patterning observed in chemotactically moving cells is induced by an external cue: the gradient of the chemoattractant to be followed (or of the chemorepellent to be avoided) [5,6].

Finally, even in the absence of mitosis and of external gradients, a cell can experience spontaneous symmetry-breaking in the spatial distribution of some proteins and it starts moving in random directions [7].

In both cases, it is necessary that a head-tail pattern be formed. From the biophysical point of view, both cases are classified as pattern onset in nonequilibrium systems. Patterns formation in biosystems is a fundamental topic of computational biology, and it is a most influential topic in experimental biology. This area of investigation was launched by the publication of Alan Turing's widely cited paper on morphogenesis [8], in which he modeled the onset of a pattern for two kinds of multicellular structures (a ring and a sphere) as a symmetry-breaking bifurcation driven by a strong difference in the diffusion coefficients of two morphogens. This mechanism is called the Turing bifurcation. In the early 1970s, the Turing mechanism was biologically substantiated by Gierer and Meinhardt [9–11], who introduced two possible patterning mechanisms based on the Turing bifurcation. The first is the activation-inhibition model, where the pattern is induced by the reaction-diffusion interplay between a *short range* self-activating chemical (which is membrane-bound or, in any case, has a very low diffusion coefficient) and a *long-range* inhibitor chemical (which has a far larger diffusion coefficient). The second model is the activation-depletion model, where two proteins interact: the first protein is again a short-range self-activator, but the second protein is no longer an inhibitor. On the contrary, the second protein is, instead, depleted by the activator.

*alberto.donofrio@ieo.eu

These pioneering studies generated a considerable amount of literature, which is increasingly linked with experimental data [3,12–15].

In 2005, Gamba and colleagues [16–19] proposed a stochastic model of chemotaxis-induced spatial symmetry breaking in a single cell. The core of this model was the interplay between two membrane-bound molecules and two cytosolic molecules. The presence of some feedback (with related bistability) and the difference of diffusion coefficients induced a mechanism of phase separation, which is different from the mechanisms based on Turing's bifurcation. Quite interestingly, in the supplementary materials of Ref. [16], Gamba *et al*. proposed a simplified and mean-field version of their model whose solution, in one spatial dimension, is a traveling wave whose velocity decreases until the front of the wave stops.

In 2008, Edelstein-Keshet and colleagues proposed in Refs. [20–23] a similar but simpler biomechanism leading to the onset of single-cell polarization due to the "freezing" of a traveling wave of the density of a membrane-bound protein. Indeed, this elegant and minimalist mechanism is based on the interconversion of a membrane-bound active protein "A" in its cytosolic inactive form "B," where "A" positively feedbacks on its activation. Also, this process induces the initial onset of a wavefront that stops, as in Ref. [16]. This phenomenon is called in physics "wave-pinning" [24]. The wave-pinning-induced cellular polarization will here be called WPP.

The WPP process proposed in Ref. [20] has a biological background, since it fits with the behavior of certain key proteins involved in cell polarization [20], such as Rho-GTPases, which switch between active membrane-bound and inactive cytosolic forms.

Some similarities exist between the WPP and the activation-depletion induced polarization (ADP) since: (i) in WPP the two involved molecular forms have very different diffusion coefficients; and (ii) the positive feedback of "A" on its activation that depletes "B" is remindful of the depletion mechanism. However, in WPP the patterning mechanism is totally different, since in it no Turing bifurcation is observed, and, conversely, in the Turing-based models no waves are observed. Moreover, one of the "essential ingredients" [20] of the WPP model is the presence of bistability (see also Refs. [16,18]), making it a genuinely nonlinear model, whereas the Turing bifurcation stems from the linearization of reaction-diffusion equations. Finally, in WPP the total mass of the two forms "A" and "B" is conserved.

Summarizing, from a theoretical point of view, although they are two quite different mechanisms, both ADP and WPP have equivalent effects of inducing a polarization pattern in the cell. However, passing from general principles to concrete numerical simulations in the case of realistic parameters values, in Ref. [20] it has been shown that the WPP has (at least for the examined range of parametric values) an important advantage over ADP: it is extremely rapid. Indeed, in WPP the prepatterning transient has a characteristic time of more or less 10 seconds, whereas ADP would require more than 10 minutes [20]. The latter time is too long and would make ADP unsuitable, especially for chemotaxis-driven polarization.

This temporal difference in the duration of respective transients makes WPP a very attractive mechanism to be experimentally validated.

Moreover, from the point of view of theoretical physics, the WPP model is one of few examples (see also Ref. [24]) of robust wave-pinning. Indeed, the standard wave-pinning condition is fulfilled for isolated points of a key parameter, and also for very small parametric changes the wave restarts traveling.

Very recently, a paper was published by Welther and colleagues [21] on the robustness of the WPP model with respect to the intrinsic stochasticity, i.e., by considering the fact that the molecular distribution is discrete and not continuous. The main result of the authors' investigation was that for a very small number of molecules, the wave collapses and the WPP is destroyed.

Here we study another and equally important problem: the robustness of WPP with respect to the unavoidable presence of extrinsic noise.

As mentioned above, one of the bases of WPP is the presence of multistability. The interplay between extrinsic noise and multistability is of fundamental relevance in chemistry and systems biology [25–27], as has been shown since the pioneering work by Kramers [28]. In a nonlinear system, the presence of noise may in fact cause the transition from one state to another [29] (for other important effects see Ref. [27]). This transition in the WPP case might mean that the noise could induce the switch from a polarized to a nonpolarized molecular distribution. Moreover, the presence of noise may deeply affect the dynamics of traveling waves, as reviewed in Ref. [30].

Many studies in the field of noise-induced phenomena in both zero-dimensional and in spatially extended systems were, respectively, based on temporal [31] or spatiotemporal white noises [32–35]. However, extrinsic fluctuations may exhibit both temporal and spatial structures [36,37], which may induce new effects [38–40]. These points are of interest in studying the WPP since the above-mentioned rapid duration of the transient leading to full polarization suggests that the WPP might not be sufficiently robust to realistic colored extrinsic noises representing the interplay of the WPP mini-network with other biomolecular networks that have the same or even larger characteristic times.

We investigate here these issues by means of numerical simulations of the WPP model in the important case where the external perturbations are not only non-Gaussian and spatiotemporally colored but also bounded [41]. Indeed, by imposing the boundedness of the random perturbations in a biomolecular network, the degree of realism of the model is increased since external noises must preserve the positiveness of reaction rates, and they must not be excessively large [27]. Similar requirements are needed in order to model other externally perturbed bioprocesses, such as tumor growth [42], where stochastically fluctuating parameters must remain strictly positive. These features can only be modeled by employing bounded noises.

The studies on bounded noises were initially focused on the properties and applications of Dichotomous Markov Noise (DMN) [40]. In the past 20 years, however, other classes of bounded noises were defined and intensively studied in the statistical physics [41]. As far as spatially extended systems are concerned, apart from spatial versions of DMN, only a few kinds of spatiotemporal-bounded noises were defined in

Refs. [43,44]. The deepening and development of theoretical studies on bounded noises led to the attention of a vast readership on new phenomena, such as the dependence of the noise-induced phenomena on the specific model of noise that has been adopted [41,45]. This means that, in the absence of experimental data on the density and spectrum of the stochastic fluctuations for the problem in study, a scientific work must compare multiple kinds of possible stochastic perturbations [41]. Here we adopt this approach, and we employ two of the above-mentioned spatiotemporal bounded noises: the Cai-Lin and the sine-Wiener noises [41,45], which both extend two well-known nonspatial bounded noises [46–48].

This work is organized as follows: in Secs. II and III we provide some background material on bounded noises and on the WPP model, respectively; in Sec. IV we propose the stochastic version of the WPP model, where we include spatiotemporal extrinsic perturbations; in Sec. V we illustrate and, from a biophysical perspective, comment on our numerical simulations. We then offer some concluding remarks.

II. UNBOUNDED AND BOUNDED NOISES

Let us consider the well-known zero-dimensional Ornstein-Uhlenbeck stochastic differential equation:

$$\xi'(t) = -\frac{1}{\tau_c}\xi(t) + \frac{\sqrt{2D}}{\tau_c}\eta(t), \tag{1}$$

where $\tau_c > 0$, $\sqrt{2D}$ is the noise strength, and $\eta(t)$ is a Gaussian white noise of unitary intensity $\langle \eta(t)\eta(t_1)\rangle = \delta(t - t_1)$. The solution of Eq. (1) is a Gaussian colored stochastic process with autocorrelation $\langle \xi(t)\xi(t_1)\rangle \propto \exp(-|t - t_1|/\tau_c)$. In Ref. [49], Eq. (1) was generalized in a spatially extended setting by including in it the most known and simple spatial coupling, i.e., the Laplace operator. This yielded the following partial differential Langevin equation:

$$\partial_t \xi(x,t) = D_{\text{noise}}\nabla^2\xi(x,t) - \frac{1}{\tau_c}\xi(x,t) + \frac{\sqrt{2D}}{\tau_c}\eta(x,t), \tag{2}$$

where $D_{\text{noise}} > 0$ is the spatial correlation strength [49] of $\xi(x,t)$.

Two strategies have mainly been adopted so far for defining zero-dimensional bounded noises: (i) applying nonlinear filters to unbounded noises; (ii) applying bounded functions to unbounded noises.

The first approach was employed in Refs. [46,47,50], where the following family of bounded noises was introduced:

$$\dot{\xi}(t) = -\frac{1}{\tau_c}\xi(t) + \sqrt{\frac{B^2 - \xi^2}{\tau_c(1+z)}}\eta(t), \tag{3}$$

where $\eta(t)$ is a Gaussian white noise. The bounded nature of the noise described in Eq. (3) easily follows from the fact that $\xi = +B$ $(-B)$ implies $\dot{\xi} < 0$ (>0). The process $\xi(t)$ has zero mean and the same autocorrelation of the OU process [46,47], and its stationary probability density is given by: $P_{\text{CL}}(\xi) = A(B^2 - \xi^2)_+^z$. For $z > 0$, the distribution is unimodal and centered in 0, while for $-1 < z < 0$ it is bimodal, having a "horned" distribution with two vertical asymptotes at $\xi \to \pm B$.

In order to define spatiotemporal bounded noises based on the Cai-Lin noises, in Ref. [43] we adopted an approach analogous to that employed in Eq. (2) to extend the OU process [49,51]. This yielded the following equation:

$$\partial_t \xi(x,t) = D_{\text{noise}}\nabla^2\xi(x,t) - \frac{1}{\tau_c}\xi(x,t) + \sqrt{\frac{B^2 - \xi^2}{\tau_c(1+z)}}\eta(x,t). \tag{4}$$

The sine-Wiener noise [48] is obtained by applying the bounded function $h(u) = B\sin(\sqrt{2/\tau_c}u)$ to a random walk $W(t)$ defined as $W' = \eta(t)$, where $\eta(t)$ is a Gaussian white noise of unitary intensity, yielding

$$\zeta(t) = B\sin\left[\sqrt{\frac{2}{\tau_c}}W(t)\right]. \tag{5}$$

The stationary probability density of $\zeta(t)$ is given by $P_{\text{SW}}(\zeta) = 1/(\pi\sqrt{B^2 - \zeta^2})$, thus, $P_{\text{eq}}(\pm B) = +\infty$.

In Ref. [44], as a natural spatial extension of the sine-Wiener noise, we defined the following spatiotemporal noise:

$$\zeta(x,t) = B\sin[2\pi\xi(x,t)], \tag{6}$$

where $\xi(x,t)$ is defined by Eq. (2).

Detailed studies of the properties of the above-defined spatiotemporal noises have been reported in Refs. [43,44].

III. BACKGROUND ON THE WPP MODEL

The WPP model describes the interplay of two different forms (active, "A," and inactive, "B") of a biomolecule, of which the active form is membrane-bound and the other form is located in the cytosol and has a very large diffusion coefficient. Denoting with $a(x,t)$ and $b(x,t)$, the concentrations of, respectively, "A" and "B," the WPP model reads

$$\partial_t a = D_a\nabla^2 a + f(a,b;p), \tag{7}$$

$$\partial_t b = D_b\nabla^2 b - f(a,b;p), \tag{8}$$

where D_a and D_b are the diffusion coefficients of "A" and "B," and p is a vector of parameters (see below). Since "A" is membrane-bound and "B" is free in the cytosol, the following condition must hold:

$$D_b \gg D_a. \tag{9}$$

A central hypothesis in Ref. [20] is that "A" positively feedbacks on its activation. Thus, it is assumed that $f(a,b;p)$ is of the form $g(a;p)b - h(a;p)$ with $\partial_a g(a;p) > 0$ and $\partial_a h(a;p) > 0$, where $g(a;p)$ and $h(a;p)$ are, respectively, the activation and the deactivation rates for A. Namely, in Ref. [20] the following functional form is employed:

$$f(a,b;p) = b\left(k_a + \frac{\gamma\omega a^2}{K^2 + \omega a^2}\right) - \delta a. \tag{10}$$

As a consequence, the vector of parameters reads

$$p = (k_a,\gamma,K,\omega,\delta). \tag{11}$$

The boundary conditions are assumed to be of the no-flux type:

$$\nabla a(t,0) = \nabla a(t,L) = \nabla b(t,0) = \nabla b(t,L) = 0, \tag{12}$$

which, of course, imply the mass conservation:

$$\int_0^L [a(t,x) + b(t,x)]dx = Q. \tag{13}$$

Note that the fundamental assumption $D_b \gg D_a$ ensures the correct working, and the robustness, of the wave-pinning mechanism.

In Refs. [20,52] it is assumed that $a(x,t)$, $b(x,t)$, and K are nondimensional. However, in a more recent work [21], Walther and coworkers considered the discrete version of the former model assigning a physical dimensional to all the parameters and variables. Based on experimental works [53–55], in Ref. [21]—as well as in all our simulations—the densities $a(t,x)$ and $b(t,x)$ are expressed in terms of μM and the following values for the parameters of the WPP model were adopted:

$$\begin{aligned} &D_a = 0.1\,\mu\text{m}^2\,\text{s}^{-1}, \quad D_b = 10\,\mu\text{m}^2\,\text{s}^{-1}, \quad \omega = 1, \\ &\delta = 1\,\text{s}^{-1}, \quad \gamma = 1\,\text{s}^{-1}, \quad k_a = 0.067\,\text{s}^{-1}, \\ &K = 1\,\mu\text{M}, \quad L = 10\,\mu\text{m}. \end{aligned} \tag{14}$$

By employing the above values of parameters, Mori and coworkers [20] numerically showed that the system Eqs. (7) and (8) with $f(a,b;p)$ defined by Eq. (10) can generate a polarization in response to initial transient cues and in the absence of cues. Moreover, their simulations also showed that the onset of the generated pattern is faster than in the Turing mechanism. Namely, they obtained that the time to polarize is of the order of 1 to 10 s, and the effective time to "complete the polarization" [20] is of approximately 30 s. Of course, radically different values of the parameters might induce slower or faster responses of the system.

IV. INCLUDING EXTRINSIC NOISE IN THE WPP MODEL

We phenomenologically take into the account the interplay of A and B with other unknown biomolecular networks that cannot be explicitly included in our model by introducing spatiotemporal perturbations in our baseline model. Indeed, the activation and deactivation of A modeled in Ref. [20] by the function $f(a,b;p)$ are the result of a number of other bioprocesses of greater and lesser relevance [56–58] that are not directly taken into the account in the deterministic model, which is quite standard procedure in systems biology. Namely, we assume that one of the components of the vector of the

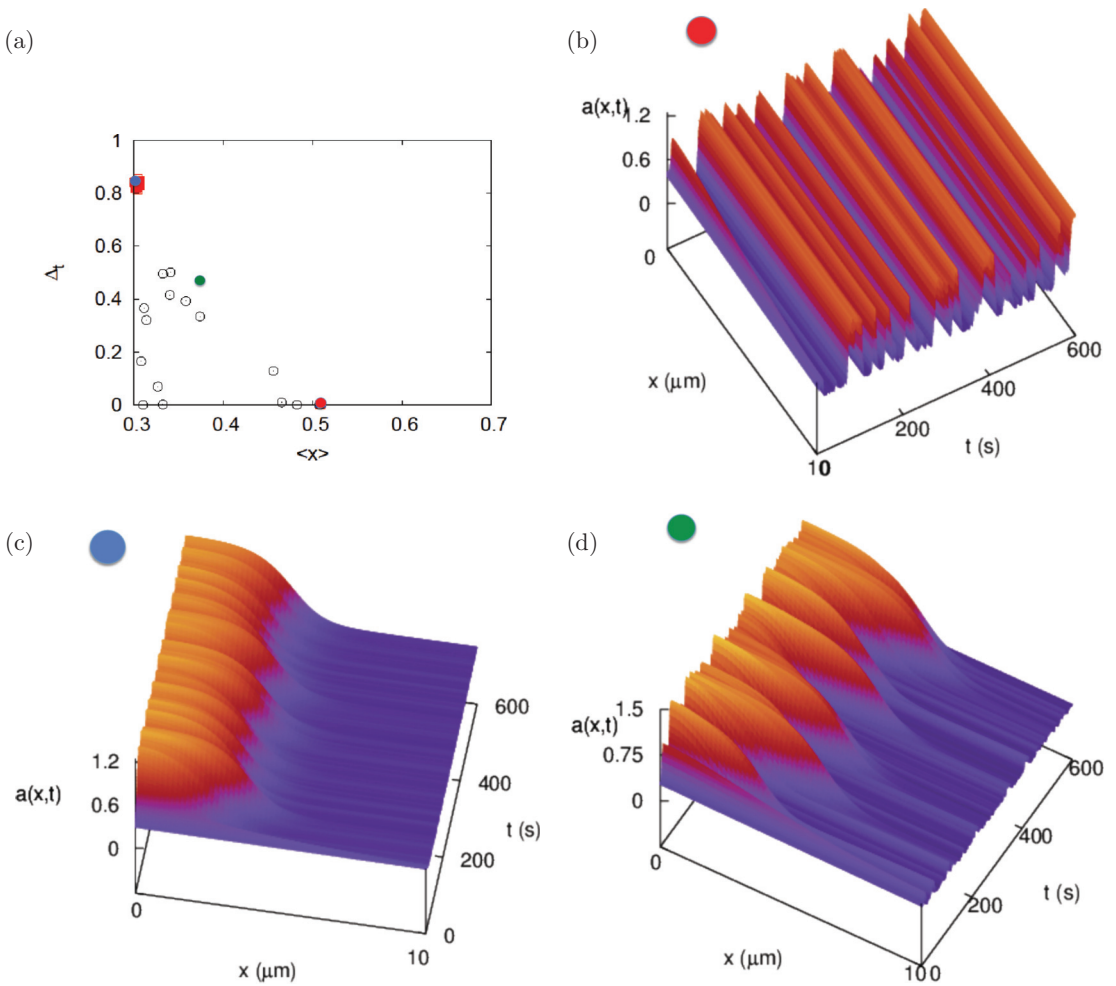

FIG. 1. (Color online) Bounded stochastic perturbation of parameter δ. Type of noise: spatially white Cai-Lin noise with temporal correlation $\tau_c = 10$ s. Panel (a): scatterplot $(\Delta_t, \langle x \rangle)$ for the density $a(x,t)$. For large and intermediate values of Δ_t the system is polarized, see panels (c) and (d), and the fluctuations of the polarization front are more pronounced for decreasing Δ_t. For $\Delta_t \simeq 0$, the system is not polarized and is characterized by a (spatially constant) temporal oscillation dynamic; see panel (b). Δ_t and $a(x,t)$ are measured in μM.

parameters p is perturbed by a spatiotemporal bounded noise. Let us suppose that the jth component of the parameter of p is perturbed by an extrinsic noise. Thus, formally we may write:

$$\partial_t a = D_a \nabla^2 a + f[a,b;\widehat{p}(x,t)] + k_S(x,t)b, \tag{15}$$

$$\partial_t b = D_b \nabla^2 b - f[a,b;\widehat{p}(x,t)] - k_S(x,t)b, \tag{16}$$

where $k_S(x,t)b$ is the initial transient cue, which is null after a short time, and $\widehat{p}(x,t)$ is the vector of the perturbed parameters whose components are:

$$\widehat{p}_i(x,t) = \begin{cases} p_i & \text{if } i \neq j \\ p_i[1+\xi(x,t)] > 0 & \text{if } i = j \end{cases}, \tag{17}$$

where $\xi(x,t)$ is a bounded noise of the Cai-Lin or sine-Wiener type. We employ two different kinds of noise in line with the recent literature on bounded noises [42–45], which in other contexts showed that the statistical characteristics of a system perturbed by a bounded stochastic process depend not only on the bound of the noise, but also on its finer structure.

Unfortunately, no analytical tools are currently available to investigate the effects of bounded spatiotemporal perturbations. We shall therefore resort to numerical simulations.

We consider two kinds of numerical experiments corresponding to, respectively, cued and uncued polarization of a cell:

(i) external graded transient cue, modeled by

$$k_S(x,t) = s(t)(1 - x/L), \tag{18}$$

$$s(t) = \begin{cases} S & t \in [0,t_1] \\ S\left(1 - \frac{t-t_1}{t_2-t_1}\right) & t \in [t_1,t_2]; \\ 0 & t > t_2 \end{cases} \tag{19}$$

(ii) random initial conditions with no external transient cue, i.e.,

$$a(x,0) = R\,\eta(x)a_-, \quad b(x,0) = 2.0, \tag{20}$$

where $a_- = 0.2683312\,\mu$M corresponds to the lower homogeneous steady state of the WPP model and $\eta(x)$ is a spatial noise uniformly distributed in $[0,1]$.

In both cases, Mori *et al.* [20] showed that the transient lasts less than 200 s, at which time it is well established. However, the presence of spatiotemporal correlations might induce slower transients; we therefore simulated all systems up to time $T = 600$ s. As a first statistical analysis measured for each realization of our stochastic process is the following:

$$\langle x \rangle = \frac{\int_0^L \frac{x}{L} a(x,T)dx}{\int_0^L a(x,T)dx}, \tag{21}$$

which is the average normalized "position" x/L weighted by the normalized version of $a(x,T)$. These statistics measure

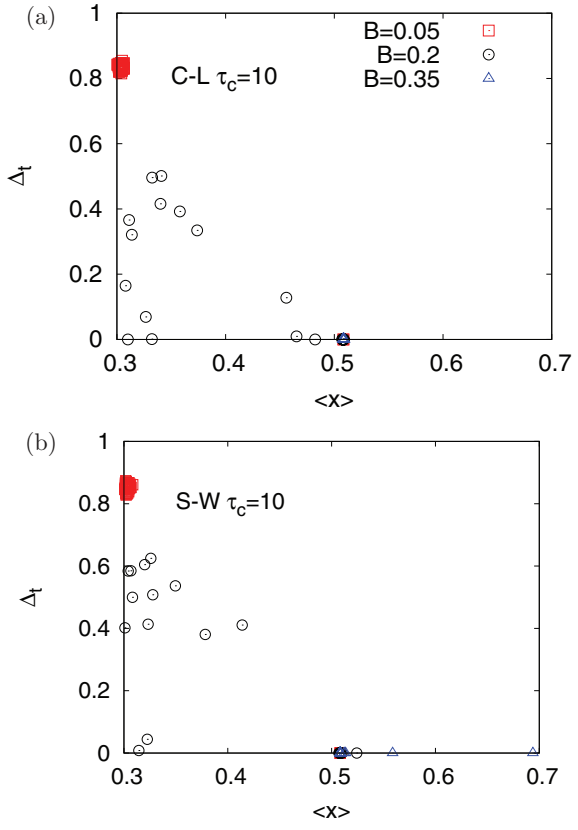

FIG. 2. (Color online) Spatially white but temporally colored perturbations of parameter δ: scatterplot $(\Delta_t, \langle x \rangle)$. (a) Cai-Lin noise; (b) sine-Wiener noise. In both cases, $\tau_c = 10$ s. Number of simulated systems is 50. Δ_t is measured in μM.

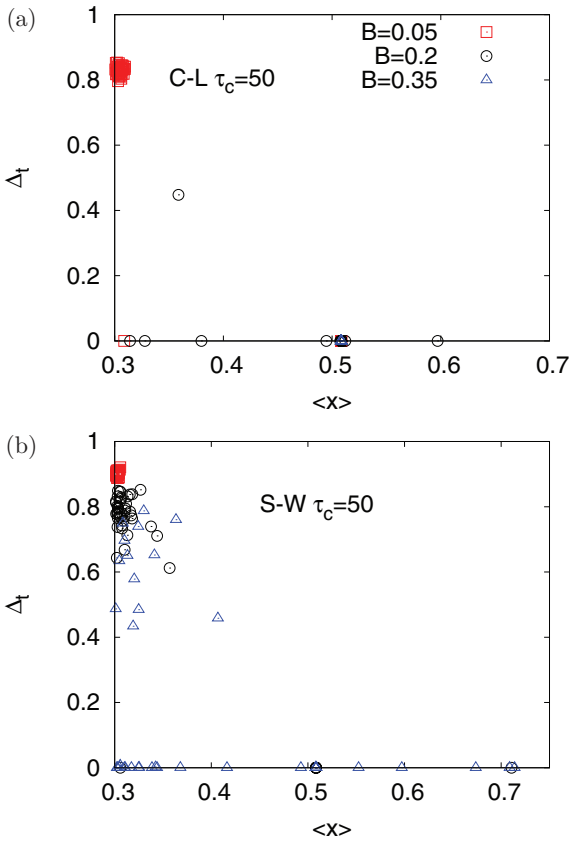

FIG. 3. (Color online) Spatially white but temporally colored perturbations of parameter δ: scatterplot $(\Delta_t, \langle x \rangle)$. (a) Cai-Lin noise; (b) sine-Wiener noise. In both cases, $\tau_c = 50$ s, $B = 0.2$. Number of simulated systems is 50. Δ_t is measured in μM.

how the polarization is oriented. Of course, in the case of cued polarization, this measure is mainly relevant to assess whether the polarization is in line with the cue, or if it is not present, in the final simulation time. The second and more important statistical analysis should then measure some variance of the density. Thus, natural candidate statistics might be the measures of the variance of the spatial concentration of A in the final simulation time. However, during our numerical simulations, we observed cases where the stochastically perturbed front became uniform and then resumed a polarized state, in some cases in an oscillating fashion. As a consequence, the analysis of the variability of the profile of a must also consider the past history of the system. Namely, based on the instantaneous "amplitude" of the distribution:

$$\delta_t = [\mathrm{Max}_{x\in[0,L]}a(x,t)] - [\mathrm{min}_{x\in[0,L]}a(x,t)], \qquad (22)$$

we defined the following statistical observable:

$$\Delta_t = \mathrm{min}_{t\in[200,T]}\delta_t. \qquad (23)$$

Note that in the case of noisy initial conditions, we expect an equiprobable distribution of the polarization and also in cases where both Δ_t is "large" and $\langle x\rangle \approx 0.5$, which indicate the presence of a "central hump" in the distribution of a.

As far as the characteristics of the employed noises are concerned, we shall assume that their temporal autocorrelation has a time scale of 10 s. Also, far larger values would be acceptable, since there is a number of biomolecular processes that are characterized by long time scales. However, in those cases the loss of polarization would be almost certain. As far as the spatial scales of the noises are concerned, we considered three cases: (i) spatially white noises; (ii) spatially uniform noises; and (iii) finite spatial correlation.

V. NUMERICAL SIMULATIONS

In this section we summarize the results of our numerical simulations, both for the case of cells stimulated by an external short-lived cue and for the case of absence of cues.

Note that for the sake of simplicity, here instead of using sentences such as "this simulation of the model suggests that the cell does something" we shall concisely write (with slight abuse of meaning) "the cell does something."

As far as the numerical methods are concerned, in all our simulations the stochastic predictor-corrector algorithm [32] for Itô partial stochastic differential equations was adopted to simulate the noise. Moreover, in the case of the Cai-Lin noise the transformation described in Ref. [43] was also adopted. The WPP model was then simulated by means of the second-order Runge-Kutta algorithm.

A. External cues

In the first round of simulations, we stimulated the system in the presence of the graded external cue, described in Eqs. (18) and (19), with $S = 0.07\,\mathrm{m\,s^{-1}}$, $t_1 = 20$ s, and

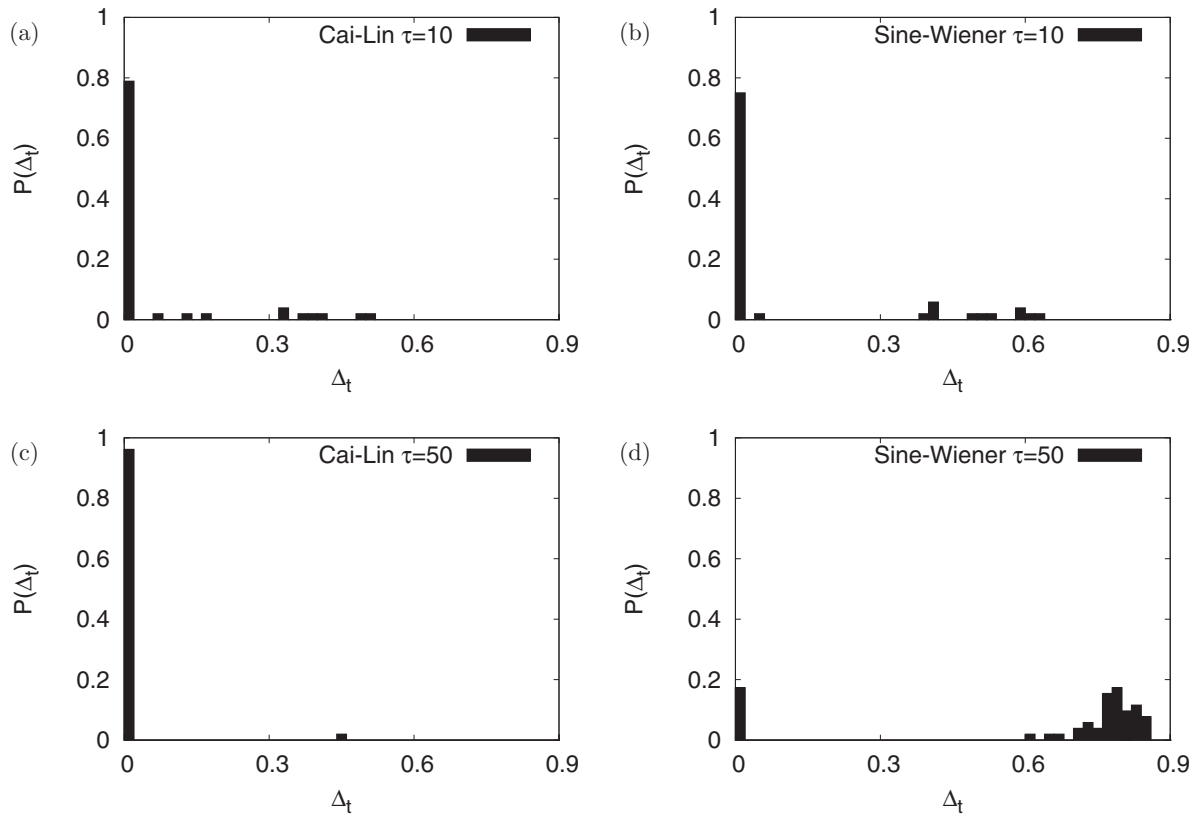

FIG. 4. Spatially white but temporally colored perturbations of parameter δ: heuristic histograms of the distributions $P(\Delta_t)$. Upper panels, $\tau_c = 10$ s; lower panels, $\tau_c = 50$ s. Panels (a) and (c), response to Cai-Lin noise; panels (b) and (d), response to sine-Wiener noise. In all panels, $B = 0.2$. The response to increasing τ_c is different for the two kinds of noises: the depolarization probability increases for Cai-Lin noise, decreases for sine-Wiener noise. Δ_t is measured in μM.

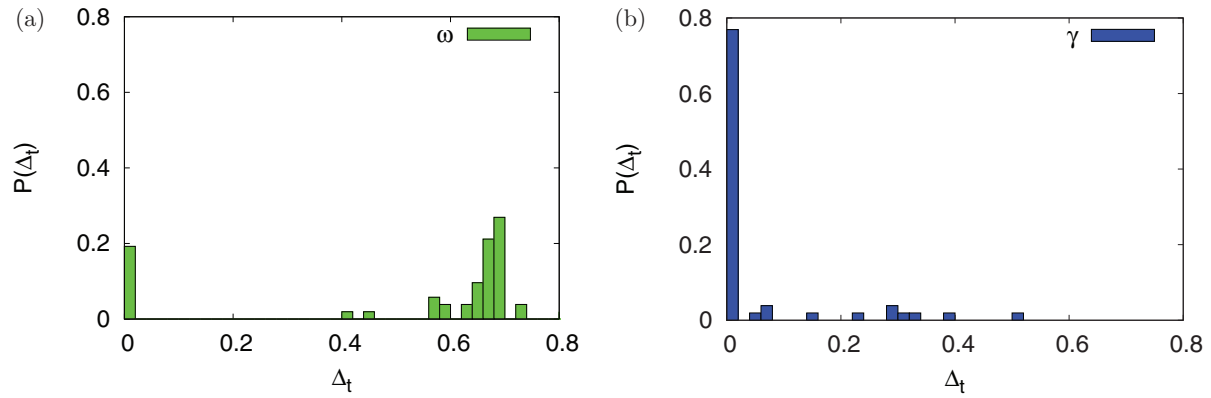

FIG. 5. (Color online) Spatially white but temporally colored perturbations affecting ω (a) and γ (b): heuristic histograms of the distributions $P(\Delta_t)$. In both cases, Cai-Lin noise with $\tau_c = 10$ s and $B = 0.2$. Δ_t is measured in μM.

$t_2 = 25$ s. The initial conditions were: $[a(x,0),b(x,0)] = (a_-,b_0) \approx (0.2683\,\mu\text{M}, 2.0\,\mu\text{M})$, corresponding to the lower homogeneous steady state of the unperturbed system [20]. In the absence of noise we obtained, as in Ref. [20], that the cell polarizes with time-scales of the order of 50 s.

By introducing an extrinsic noise into one of the relevant parameters of function $f(a,b)$ via Eq. (17), we obtained a complex pattern of responses, dependent upon the spatial and temporal parameters of the noise, as well as of its type.

In some cases, which we shall illustrate, our stochastic model predicts that the cell polarization is preserved, although, of course, the wave-front experiences some random fluctuations; in other cases the cell depolarizes. In these cases, the profile of the concentration of A is flat and oscillating.

In no case was an inversion of the polarization observed, i.e., the polarized state followed the external cue in all cases.

Typical configurations are shown in Fig. 1, where both a scatterplot $(\Delta_t, \langle x \rangle)$ and three specific realizations are shown.

We now illustrate the statistical response of the model to bounded perturbations that are spatially white, i.e., $D_{\text{noise}} = 0$.

Initially, we shall consider perturbations in the parameter δ.

In such a case, we observed that the response to the noise strongly depends on the type of the perturbation. Indeed, setting $\tau_c = 10$ s and $B = 0.2$, both Cai-Lin and sine-Wiener noises cause depolarization of the cell in many cases. This is illustrated by the scatterplots shown in Fig. 2, and in the distribution of Δ_t shown in the upper panels of Fig. 4.

By increasing the temporal autocorrelation τ_c up to 50 s, we observed two dichotomous behaviors. If the perturbation is a Cai-Lin noise then the increase of τ_c causes a larger number of depolarizations [see Figs. 3(a) and 4(c)]. Conversely, if the bounded noise is of sine-Wiener type, then one observes a larger probability that the cell maintains the polarization induced by the external deterministic cue [see Figs. 3(b) and 4(d)].

As far as perturbations in ω and γ are concerned, fluctuations in γ induce effects comparable to the ones caused by noises affecting δ, whereas perturbations of ω depolarize to a lesser extent (Fig. 5). Note that the perturbation of ω may summarize the effect of extrinsic noise in the feedback mechanism.

We now examine the effects of spatially correlated noises. In Figs. 6 and 7, we show that the presence of non-null spatial correlation, i.e., $D_{\text{noise}} > 0$, increases not only the probability of maintaining the cell polarization, but also its intensity (i.e., the magnitude of spatial gradient of a). Indeed, in such cases simulations suggest not only a decrease of the probability of observing small or null Δ_t, but also a significant increase of the probability that Δ_t is "large." For example, if $D_{\text{noise}} = 0.01$ the probability $P(0)$ is quite large (in 30% of cases the cell is not polarized), whereas for $D_{\text{noise}} \geqslant 0.1$ $P(0)$ is small and it is a decreasing function of D_{noise}.

We also simulated the response of the WPP model to a noise that is spatially uniform but temporally varying. Namely: (i) instead of the spatiotemporal Cai-Lin noise, we used a noise $\beta(x,t) = \xi(t)$, where $\xi(t)$ is the temporal Cai-Lin noise; (ii) instead of the sine-Wiener noise we employed a noise $\beta(x,t) = B\sin[2\pi\xi(t)]$, where $\xi(t)$ is the OU noise. Since in this case the spatial correlation length is infinite, we expected to observe that all the simulated cells could maintain their polarization. Quite interestingly, we observed that this spatially uniform noise induces [see Fig. 7(f)] in the model a behavior that is comparable to that induced by spatially white noises [compare with previous Fig. 7(a)].

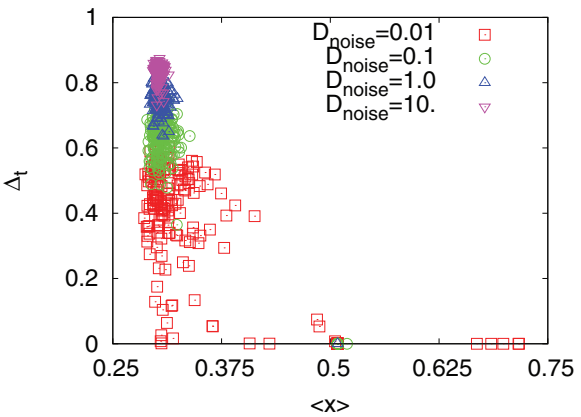

FIG. 6. (Color online) Spatially and temporally colored noise: scatterplot $(\Delta_t, \langle x \rangle)$ for various values of D_{noise}. Here the perturbed parameter is γ. Type of noise is Cai-Lin. Parameters $\tau_c = 10$ s, $B = 0.2$. Number of points for each series is 200. Δ_t is measured in μM.

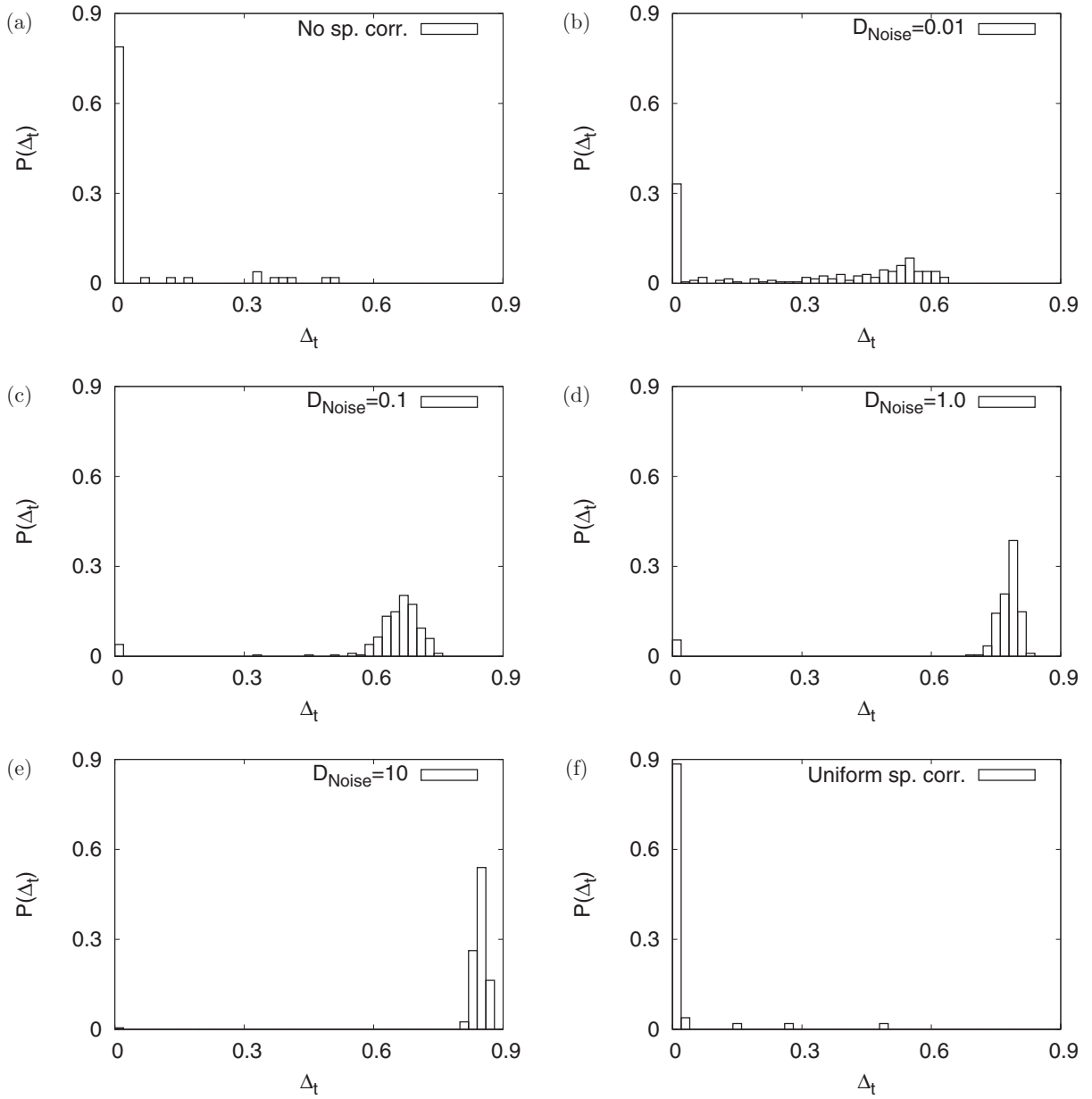

FIG. 7. Histograms of $P(\Delta_t)$ in case of various degrees of spatial correlation of a Cai-Lin perturbation applied to parameter δ. Panel (a), $D_{\text{noise}} = 0$; panel (b), $D_{\text{noise}} = 0.01$; panel (c), $D_{\text{noise}} = 0.1$; panel (d), $D_{\text{noise}} = 1$; panel (e), $D_{\text{noise}} = 10$; panel (f), spatially uniform noise. Other parameters: $\tau_c = 10$ s, $B = 0.2$. Δ_t is measured in μM.

B. Initial random state

Here we illustrate the results of simulations performed without adding the external deterministic cue, but considering an initial random distribution of A, following Eq. (20) with $R = 3$.

In the absence of noise, we observed three possible kinds of steady states: polarization (left or right, in this case it does not matter) or a central "hump."

As far as spatially white noises are concerned, we observed a behavior depending on the perturbed parameter but not on the type of noise. Indeed:

(i) in the case of perturbation of δ (see Fig. 8, where the noise is of sine-Wiener type): for $B = 0.2$, solutions with central hump are not observed, and in some cases the cell is not polarized. Absence of polarization is always observed if $B = 0.35$;

(ii) in the case of perturbation of ω (see Fig. 9) or of γ (not shown): for $B = 0.2$, cells seldom are not polarized and the number of solutions with central "hump" is roughly similar to that observed if $B = 0.05$. For $B = 0.35$, in some cases the cells remain polarized (and no cells have the "hump" pattern).

Finally, also here the increase of spatial correlation restores the polarization.

VI. CONCLUDING REMARKS

Our main aim in this work was to study the robustness to extrinsic stochasticity of an interesting mechanism explaining

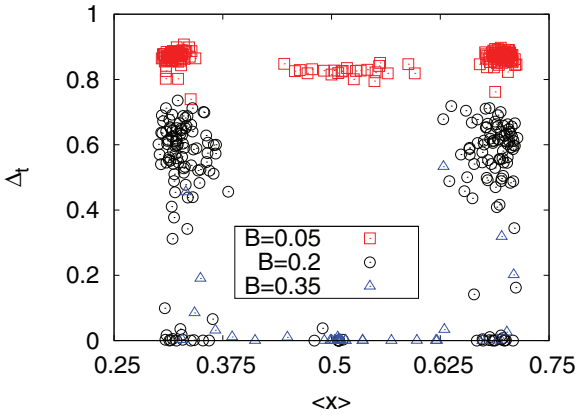

FIG. 8. (Color online) Random initial conditions and spatially white sine-Wiener perturbation of δ. Scatterplot $(\Delta_t, \langle x \rangle)$ for three values of B. Other parameters: $\tau_c = 10$ s. Δ_t is measured in μM.

both cued and uncued cellular polarization: the wave-pinning [20].

We modeled the above-mentioned extrinsic perturbations by means of spatiotemporal bounded noises that model perturbations in a more realistic way than do Gaussian noises, which are unbounded. In particular, we adopted the following two noises: the Cai-Lin [43] and the sine-Wiener [44] noises, which we recently proposed.

The robustness of the WPP model to extrinsic noise was, in particular, investigated by means of suitable statistics summarizing the polarization probability, the fluctuations, and the intensity of the polarization.

An interesting feature of the deterministic WPP model is that it is deterministically robust, in the sense that most models exhibiting the wave-pinning phenomenon are such that the waves "freeze" for a specific isolated value of a given parameter [20,24]. However, in the WPP model, the system self-regulates and the wave freezes for an entire range of the chosen bifurcation parameter [20].

Here we have shown that under extrinsic stochastic perturbations, the maintenance or loss of polarization strongly depends on both spatial and temporal colors, as well as on the specific kind of noise.

Indeed, in the case of Cai-Lin noise, the increase of temporal correlation induces a decrease of polarization probability, whereas in the case of sine-Wiener noise one observes the opposite phenomenon.

Moreover, in both cases, the passing from white to spatially correlated noise induces a loss of polarization. However, in the simulations where we employed a spatially constant noise we again obtained a large probability of polarization.

In other words, the WPP model exhibits a sort of contrast of colors (the spatial and the temporal) and of noise types.

Concerning the possible use of the WPP model to describe the spontaneous cellular polarization emerging from random initial conditions, in addition to the polarized and global oscillating states, we observed (in line with Ref. [20]) the emergence of "nonpolar" patterns that are characterized by a hump in the density of A, located in the center of the cell. Moreover, the effect of the amplitude of the noise (and of the spatial coupling) is "nonmonotone." Indeed, it is possible to find an intermediate amplitude of the noise (or spatial coupling strength) by which both the probabilities

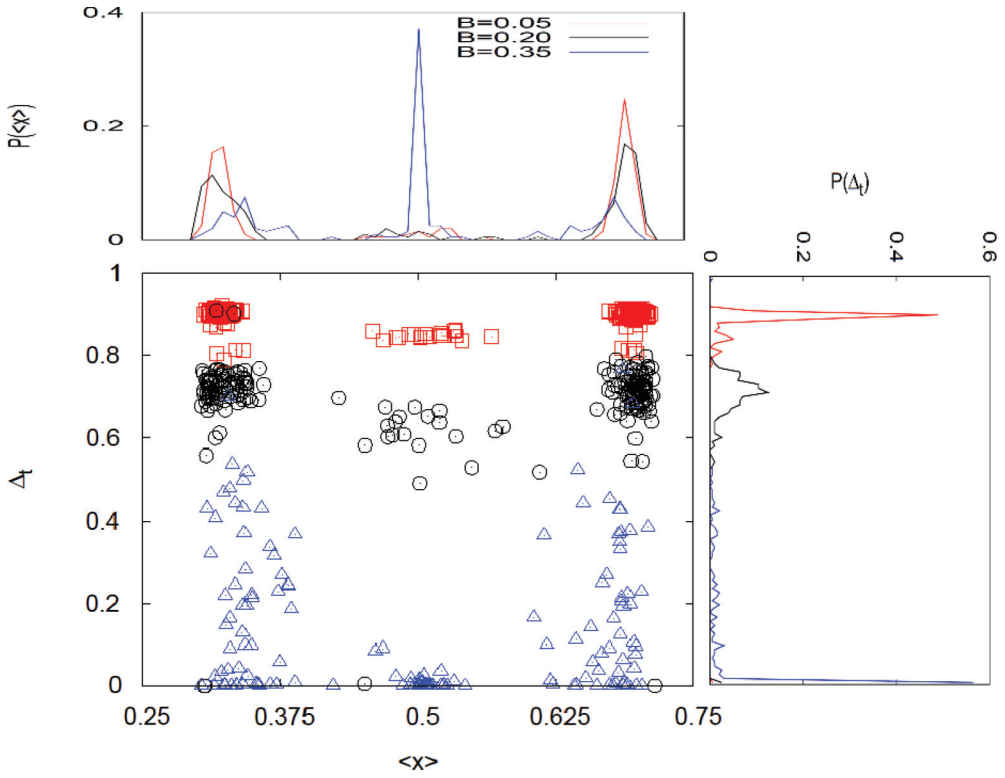

FIG. 9. (Color online) Random initial conditions and spatially white Cai-Lin perturbation of ω. Scatterplot $(\Delta_t, \langle x \rangle)$ and corresponding histograms of the distributions $P(\Delta_t)$ and $P(\langle x \rangle)$. Other parameters: $\tau_c = 10$ s. Δ_t is measured in μM.

of unpolarized oscillating states and of "humped" states are low.

Summarizing the above observations, we may say that the answer to the main substantive question—Is the WPP model robust?—is "It depends on the context in which the cell is embedded." In other words, the amplitude of the external perturbations being equal, the robustness of the wave-pinning-based mechanism of cellular polarity strongly depends on the kind of extrinsic stochasticity that affects the WPP network. Note also that the ability of this mechanism to describe a spontaneous cellular polarization is questionable (as also stressed in Ref. [22]) because of the presence of humped solutions. Nonetheless, in the presence of extrinsic noise the hump may disappear; however, in such cases the onset of noise-induced spatially homogeneous states is observed.

Regarding the onset of wave-pinning-induced polarization in the case of a low number of molecules, studied in Ref. [21], we remind the reader that for a moderate number of molecules a stochastic reaction system may be approximated by the corresponding deterministic system plus suitable multiplicative external white Gaussian noises. This is a well-known result in statistical and chemical physics [59], also known in systems biology as the "chemical Langevin equation" method [60]. Thus, here we might be tempted to interpret the results of Ref. [21] as fragility of the WPP mechanism to white noise perturbations. However, we stress here that for computational reasons the simulations of Ref. [21] were performed by assuming that the number of molecules of the species B is spatially homogeneous. Moreover, we recall that it is Eq. (8) that guarantees the robustness of WPP model. This might imply that the stochastic version of WPP model could be more robust than has been reported in the numerical simulations of Ref. [21].

Thus, our aim is, in a future work, to explore the full discrete stochastic version of Eqs. (7) and (8), also including extrinsic noises. Indeed, the interplay of intrinsic and bounded extrinsic noise may be of interest in the field of systems biology, as stressed in Ref. [27].

Finally, it is important to note that the experimental study of the role of stochastic fluctuations in the onset of intracellular patterns is in its infancy. Indeed, to the best of our knowledge only a limited number of works have been published in this field. For example, in Ref. [16] some experimental data were used to validate their mathematical model, which included extrinsic stochasticity. Recently, in Refs. [61,62] some experiments were performed to validate the prediction of two mathematical models that takes into account the spatial stochasticity in the gradient to be followed by the cells. The role of the stochastic receptor-ligand interaction during chemotaxis has been recently experimentally investigated in Ref. [63]. No experiments have been performed so far in order to investigate the role of extrinsic noise in the reaction-diffusion mechanisms determining cellular polarization. As a consequence, we have to stress that our work must be assumed to be speculative and therefore needs experimental confirmation. The aim of our work is to trigger such investigation.

ACKNOWLEDGMENT

This work was conducted within the framework of the Integrated Project P-medicine from data sharing and integration via VPH models to personalized medicine (Project No. 270089), which is partially funded by the European Commission under the Seventh Framework Programme.

[1] M. D. Onsum and C. V. Rao, Curr. Opin. Cell Biol. **21**, 74 (2009).
[2] A. Macieira-Coelho, *Asymmetric Cell Division* (Springer, Berlin, 2007).
[3] M. Sohrmann and M. Peter, Trends Cell Biol. **13**, 526 (2003).
[4] P. Ortoleva and J. Ross, Biophys. Biophys. Chem. **1**, 87 (1973).
[5] J. D. Murray, *Mathematical Biology* (Springer, Berlin, 2002).
[6] P. A. Iglesias and P. N. Devreotes, Curr. Opin. Cell Biol. **20**, 35 (2008).
[7] J. van der Gucht and C. Sykes, Cold Spring Harbor Perspect. Biol. **1**, 1 (2009).
[8] A. M. Turing, Phil. Trans. R. Soc. Lond. B **237**, 37 (1952).
[9] A. Gierer and H. Meinhardt, Kybernetik **12**, 30 (1972).
[10] H. Meinhardt, *Models of Biological Pattern Formation* (Academic Press, London, 1982).
[11] H. Meinhardt, J. Cell. Sci. **112**, 2867 (1999).
[12] H. Meinhardt, Interface Focus **2**, 407 (2012).
[13] P. K. Maini, T. E. Woolley, R. E. Baker, E. A. Gaffney, and S. S. Lee, Interface Focus **2**, 487 (2012).
[14] D. E. Strier and S. Ponce Dawson, PLoS ONE **2**, e1053 (2007).
[15] A. Mogilner, J. Allard, and R. Wollman, Science **336**, 175 (2012).
[16] A. Gamba, A. de Candia, S. Di Talia, A. Coniglio, F. Bussolino, and G. Serini, Proc. Natl. Acad. Sci. USA **102**, 16927 (2005).
[17] A. Gamba, I. Kolokolov, V. Lebedev, and G. Ortenzi, Phys. Rev. Lett. **99**, 158101 (2007).
[18] A. Gamba, I. Kolokolov, V. Lebedev, and G. Ortenzi, J. Stat. Mech.: Theory Exp. (2009) P02019.
[19] M. Semplice, A. Veglio, G. Naldi, G. Serini, and A. Gamba, PLoS ONE **7**, e30977 (2012).
[20] Y. Mori, A. Jilkine, and L. Edelstein-Keshet, Biophys. J. **94**, 3684 (2008).
[21] G. R. Walther, Athanasius F. M. Marée, L. Edelstein-Keshet, and V. A. Grieneisen, Bull. Math. Biol. **74**, 2570 (2012).
[22] A. Jilkine and L. Edelstein-Keshet, PLoS Comput. Biol. **7**, e1001121 (2011).
[23] Y. Mori, A. Jilkine, and L. Edelstein-Keshet, SIAM J. Appl. Math. **71**, 1401 (2011).
[24] J. A. Sepulchre and V. I. Krinsky, Chaos **10**, 826 (2000).
[25] S. Dasmahapatra, in *New Frontiers of Network Analysis in Systems Biology*, edited by A. Ma'ayan and B. D. MacArthur (Springer, Netherlands, 2012), pp. 31–58.
[26] B. J. Daigle, Jr., B. S. Srinivasan, J. A. Flannick, A. F. Novak, and S. Batzoglou, in *Systems Biology for Signaling Networks*, *Systems Biology*, Vol. 1, edited by S. Choi (Springer, New York, 2010), pp. 13–73.
[27] G. Caravagna, G. Mauri, and A. d'Onofrio (unpublished).
[28] H. Kramers, Physica **7**, 284 (1940).
[29] P. Jung, P. Hänggi, and F. Marchesoni, Phys. Rev. A **40**, 5447 (1989).
[30] D. Panja, Phys. Rep. **393**, 87 (2004).

[31] W. Horsthemke and R. Lefever, *Noise-Induced Transitions: Theory and Applications in Physics, Chemistry, and Biology* (Springer, Berlin, 1983).
[32] F. Sagués, J. M. Sancho, and J. García-Ojalvo, Rev. Mod. Phys. **79**, 829 (2007).
[33] Q. Y. Wang, Q. S. Lu, and G. R. Chen, Physica A: Stat. Mech. Appl. **374**, 869 (2007).
[34] Q. Y. Wang, Q. S. Lu, and G. R. Chen, Eur. Phys. J. B—Condensed Matter Complex Syst. **54**, 255 (2006).
[35] Q. Y. Wang, M. Perc, Q. S. Lu, S. Duan, and G. R. Chen, Int. J. Mod. Phys. B **24**, 1201 (2010).
[36] J. García-Ojalvo and J. M. Sancho, *Noise in Spatially Extended Systems* (Springer, Berlin, 1996).
[37] J. Sancho, J. García-Ojalvo, and H. Guo, Physica D: Nonlin. Phenom. **113**, 331 (1998).
[38] H. S. Wio and K. Lindenberg, AIP Conf. Proc. **658**, 1 (2002).
[39] P. Jung and P. Hänggi, Phys. Rev. A **35**, 4464 (1987).
[40] L. Ridolfi, P. DOdorico, and F. Laio, *Noise-induced Phenomena in the Environmental Sciences* (Cambridge University Press, Cambridge, 2011).
[41] *Bounded Noises in Physics, Biology, and Engineering*, edited by A. d'Onofrio (Springer, New York, 2013).
[42] A. d'Onofrio and A. Gandolfi, Phys. Rev. E **82**, 061901 (2010).
[43] S. de Franciscis and A. d'Onofrio, Phys. Rev. E **86**, 021118 (2012).
[44] S. de Franciscis and A. d'Onofrio, Nonlinear Dynamics (2013), doi: 10.1007/s11071-013-0992-7.
[45] A. d'Onofrio, Phys. Rev. E **81**, 021923 (2010).
[46] G. Q. Cai and Y. K. Lin, Phys. Rev. E **54**, 299 (1996).
[47] G. Cai and Y. Suzuki, Nonlin. Dynam. **45**, 95 (2006).
[48] R. V. Bobryk and A. Chrzeszczyk, Physica A: Stat. Mech. Appl. **358**, 263 (2005).
[49] J. García-Ojalvo, J. M. Sancho, and L. Ramírez-Piscina, Phys. Rev. A **46**, 4670 (1992).
[50] G. Cai and C. Wu, Probabilistic Eng. Mech. **19**, 197 (2004).
[51] J. García-Ojalvo, J. Sancho, and L. Ramírez-Piscina, Phys. Lett. A **168**, 35 (1992).
[52] A. Jilkine, Ph.D. thesis, The University of British Columbia, 2009.
[53] B. Zhang and Y. Zheng, Biochemistry **37**, 5249 (1998).
[54] Y. Sako, K. Hibino, T. Miyauchi, Y. Miyamoto, M. Ueda, and T. Yanagida, Single Mol. **1**, 159 (2000).
[55] M. Postma, L. Bosgraaf, H. M. Loovers, and P. J. M. Van Haastert, EMBO Rep **5**, 35 (2004).
[56] L. Kozubowski, K. Saito, J. M. Johnson, A. S. Howell, T. R. Zyla, and D. J. Lew, Curr. Biol. **18**, 1719 (2008).
[57] A. F. M. Marée, A. Jilkine, A. Dawes, V. A. Grieneisen, and L. Edelstein-Keshet, Bull. Math. Biol. **68**, 1169 (2006).
[58] A. Jilkine, A. F. M. Marée, and L. Edelstein-Keshet, Bull. Math. Biol. **69**, 1943 (2007).
[59] N. G. van Kampen, *Stochastic Processes in Physics and Chemistry* (North-Holland, Amsterdam, 1990).
[60] D. T. Gillespie, J. Chem. Phys. **113**, 297 (2000).
[61] C. S. Chou, L. Bardwell, Q. Nie, and T. M. Yi, BMC Syst. Biol. **5**, 196 (2011).
[62] W. C. Lo, M. E. Lee, M. Narayan, C. S. Chou, and H. O. Park, PLoS ONE **8**, e56665 (2013).
[63] J. M. Dyer, N. S. Savage, M. Jin, T. R. Zyla, T. C. Elston, and D. J. Lew, Curr. Biol. **23**, 32 (2013).